Aryl-X Bond-Forming Reductive Elimination from High-Valent Mn-Aryl Complexes

Abir Sarbajna,[†,§] Yu-Tao He,[†,§] Minh Hoan Dinh,[†] Olga Gladkovskaya,[†] S. M. Wahidur Rahaman,[†] Ayumu Karimata,[†] Eugene Khaskin,[†] Sébastien Lapointe,[†] Robert R. Fayzullin,[‡] and Julia R. Khusnutdinova*,[†]

[†]Coordination Chemistry and Catalysis Unit, Okinawa Institute of Science and Technology Graduate University, 1919-1 Tancha, Onna-son, Okinawa, 904-0495 Japan.

[‡]Arbuzov Institute of Organic and Physical Chemistry, FRC Kazan Scientific Center, Russian Academy of Sciences, 8 Arbuzov Street, Kazan 420088, Russian Federation.

ABSTRACT: C-X bond reductive elimination and oxidative addition are key steps in many catalytic cycles for C-H functionalization catalyzed by precious metals; however, engaging first row transition metal in these overall 2e⁻ processes remains a challenge. Although high-valent Mn aryl species have been implicated in Mn-catalyzed C-H functionalization, the nature and reactivity of such species remain unelucidated. In this work, we report rare examples of stable, cyclometalated monoaryl Mn^{III} complexes obtained through clean oxidative addition of Ar-Br to Mn^{I}(CO)$_5$Br. These isolated Mn^{III}-Ar complexes undergo unprecedented 2e⁻ reductive elimination of Ar-X (X = Br, I, CN) bond and Mn^{II} induced by 1e⁻ oxidation, presumably via transient reactive Mn^{IV} species. Mechanistic studies suggest a non-radical pathway.

INTRODUCTION

Transition-metal (TM) mediated C-heteroatom oxidative addition (OA) and reductive elimination (RE) are key steps in many catalytic C-H bond functionalization and C-C coupling reactions.[1-3] Given that these areas have long been dominated by precious metal catalysts such as Pt, Pd, Ir, Rh,[4-7] mechanistic understanding of C-X bond cleavage and formation steps is mostly based on the studies of stable diamagnetic 2nd and 3rd row TM complexes.[8-16] At the same time, replacement of precious metals with more abundant, cheaper and less toxic 1st row TM is an important goal in developing sustainable methods for organic synthesis.[17] Manganese complexes have recently emerged as competent catalysts for C-H bond functionalization and C-C coupling reactions.[18-26] While understanding of OA and RE from 1st row metal complexes is necessary for further development of new catalytic methods,[27-28] studying fundamental reactivity of organometallic Mn complexes remains a challenge due to their low stability, paramagnetism and a large range of common oxidation states available for this metal.[26, 29-30] Although some recent reports focus on the mechanistic studies of C-C or C-heteroatom coupling at the paramagnetic Fe[31-33] and Ni[34-37] complexes, Mn complexes remain essentially unexplored. Examples of well-defined, two-electron OA and RE of aryl-X at Fe,[38-40] or Co,[41-42] are exceedingly rare and to the best of our knowledge non-existent for Mn.[27-28] At the same time, Ar-heteroatom bond cleavage and formation are essential steps in several catalytic or stoichiometric processes developed for inexpensive 1st row transition metals, such as copper[43-46] and nickel.[47-51]
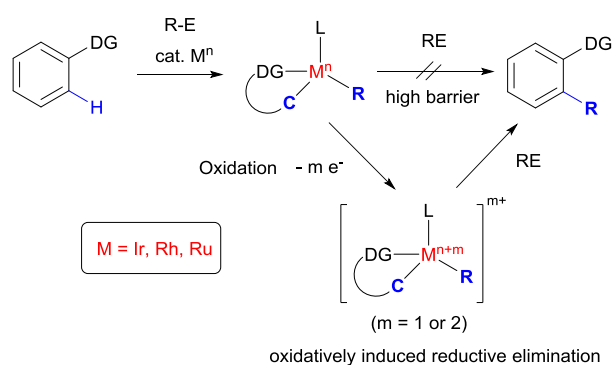
While the majority of Mn-catalyzed C-H functionalization reactions have been proposed to occur via Mn^{I} without a change in the formal oxidation state,[18, 52] the intermediacy of Ar-Mn^{III} or Ar-Mn^{IV} has also been implicated, albeit without direct experimental evidence.[22, 53-56] Mn-catalyzed halogenation and azidation of C(sp^3)-H bonds were proposed to involve an outer-sphere alkyl radical reaction with a high valent Mn^{IV} and Mn^{V} species,[57-61] however, such methodology is not applicable to Ar-X bond formation. Given the well-known ability of Mn^{I} complexes to activate Ar-H bonds in substrates containing coordinating directing groups,[17-18, 29] understanding the factors influencing selective Ar-X bond formation and cleavage would take full advantage of manganese's ability to adopt a variety of oxidation states and would shed light on the mechanism of C-H functionalization and related Ar-X bond forming reactions.

In this work, we report stable cyclometalated aryl-Mn^{III} complexes with a ^{tBu}N3C⁻ ligand formed via oxidative addition of an Ar-Br bond to a Mn^{I} precursor (Scheme 1). These Mn^{III} monoaryl complexes react readily with a range of 1e⁻ oxidants, which leads to facile, oxidatively-induced reductive elimination of an Ar-X (X = Br, I, CN) bond and a Mn^{II} product at room temperature. Mechanistic tests imply that the Ar-Br reductive elimination occurs via a non-radical mechanism, presumably via an Ar-Mn^{IV} intermediate. Overall, this study demonstrates the importance of tuning the oxidation state of Mn to achieve either OA or RE beyond a simple two-electron cycle. This parallels the concept of oxidatively induced reductive elimination (ORE) applied predominantly for catalysis by precious metals[62-66] (Scheme 2) and less commonly for 1st row TM such as Ni.[49, 67-70]

Scheme 1. Oxidative addition and reductive elimination of Ar-X using (^{tBu}N3C)Mn monoaryl complexes.
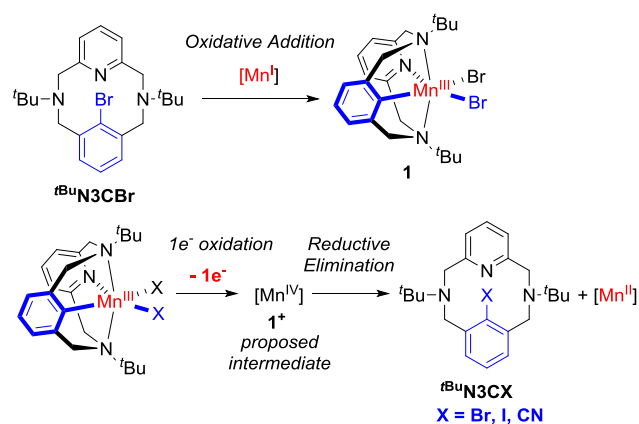
Scheme 2. The concept of oxidatively induced reductive C-C elimination from precious metal catalysts of C-H bond functionalization.[62-63]

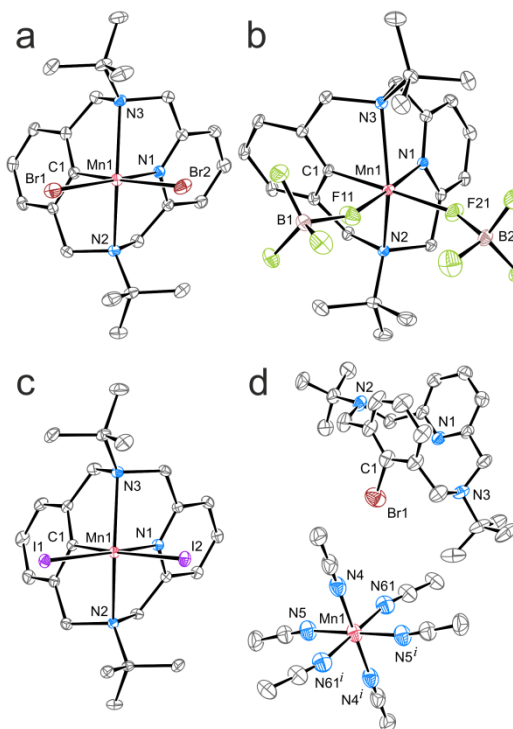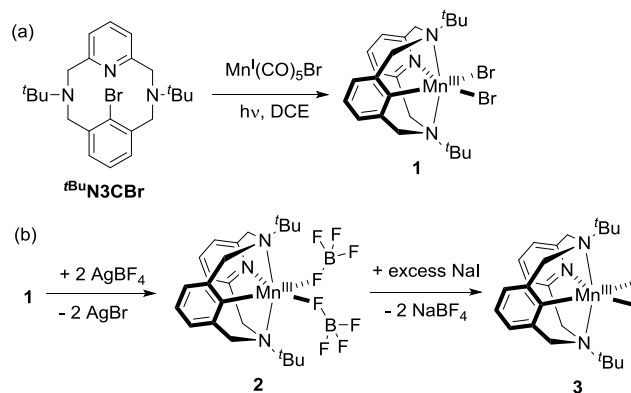**Scheme 3. Synthesis of complexes 2 and 3.**

Figure 1. ORTEP of neutral complexes **1** (a), **2** (b), **3** (c) and co-crystal of free ligand ^{tBu}**N3CBr** and hexakis(acetonitrile)manganese(II) complex (d) at 50 % probability level according to single crystal X-ray diffraction data. Hydrogen atoms (a-d), minor disordered components (a, b, d), counterions (d) and solvent molecules (b, d) are omitted for clarity; equivalent atoms are labelled by the superscript i ($-x+1$, $-y$, $-z+1$). Selected interatomic distances [Å]: Br1–Mn1 2.4623(4), Br2–Mn1 2.4793(5), Mn1–C1 2.027(14), Mn1–N1 2.063(11), Mn1–N2 2.474(2), Mn1–N3 2.445(2) for **1**; Mn1–F11 2.0483(9), Mn1–F21 2.0281(9), Mn1–C1 2.012(5), Mn1–N1 2.031(4), Mn1–N2 2.3641(11), Mn1–N3 2.3696(11) for **2**; I1–Mn1 2.6556(3), I2–Mn1 2.7461(3), Mn1–C1 2.0323(18), Mn1–N1 2.0678(16), Mn1–N2 2.4906(16), Mn1–N3 2.5032(17) for **3**.

RESULTS AND DISCUSSION

The tetradentate cyclophane-based ligand ^{tBu}N3C$^-$ ligand was selected as the convenient platform to study C-heteroatom bond formation due to its ability to stabilize high-valent species through chelation thus providing insight into the mechanisms of these reactions.[35, 71-74] At the same time, amines and pyridine donors resemble common directing groups used in chelation-assisted C-H bond activation.[75] Non-innocent character of such ligands has also been demonstrated by Ribas and co-workers in the corresponding Co complexes.[76-78] To access Ar-Mn^{III} complexes, a 1:1 mixture of Mn(CO)$_5$Br and ^{tBu}N3CBr was reacted in a dichloroethane solution at RT under Hg lamp irradiation to remove CO (Scheme 3, a). An intense red-colored solution was obtained, from which (^{tBu}N3CBr)Mn^{III}Br$_2$ (**1**) was isolated in 58% yield as a deep-red, crystalline solid (Scheme 3, a). The product was characterized by single crystal X-ray diffraction (Figure 1a), ^{1}H NMR, UV-vis and FT-IR spectroscopies, HR-MS and elemental analysis. The X-ray structure of **1** (Figure 1a) reveals a distorted octahedral geometry at the Mn center surrounded by three N-donors, two Br and an aryl ligand with a Mn-C$_{ipso}$ bond distance of 2.027(14) Å. HR-MS of **1** gives rise to a signal at 484.1149 ($z = 1$) assigned to [**1**-Br]$^+$. The complex was stable in the solid state at RT for at least one month. Complex **1** is paramagnetic with an effective magnetic moment μ_{eff} of 4.98 μ_B in solution as determined by the Evans method in CH$_2$Cl$_2$, suggesting an $S = 2$ ground state attributed to a high spin d^4 configuration. Accordingly, the magnetic

susceptibility measurement for the solid sample of **1** gives a $\chi_M \cdot T$ value of 2.7-2.9 T·cm^3·mol^{-1} in the temperature range from *ca.* 10 K to 300 K, corresponding to a μ_{eff} of 4.7-4.8 μ_B expected from a high spin d^4 Mn^{III} complex.[79]

We also obtained two other Ar-Mn^{III} complexes via initial Br abstraction with 2 equivalents of AgBF$_4$, which leads to the formation of complex **2** with BF$_4$ ligands bound through the F atoms (Scheme 3, b). Complex **2** is stable is CH$_2$Cl$_2$ solution for at least 24 hours, but undergoes decomposition upon solvent removal and prolonged exposure to vacuum. X-ray structure reveals κ^1-coordination of the two BF$_4$ anions to a Mn center via F-atoms, with Mn1-F11 and Mn1-F21 bond distances of 2.0483(9) Å and 2.0281(9) Å, respectively. Examples of Mn complexes with a κ^1-coordinated BF$_4$ ion are exceedingly rare, with only three structurally characterized Mn^I and Mn^{II} complexes reported in the literature,[79-81] although examples with other transition metal complexes are known (for selected examples, see Refs [82-86]). The B-F distances for metal-bound B-F bonds are significantly elongated (B1-F11 1.4711(17) Å and B2-F21 1.4778(17) Å) compared to the terminal B-F$_{term}$ bond distances (*ca.* 1.38 Å). As previously proposed for a similar Mn^I(κ^1-BF$_4$) complex, **2** can be formulated as having (**^{t}BuN3C**)Mn^{III}F$_2$·(BF$_3$)$_2$ adduct character.[79]

Further treatment of **2** with slight excess of NaI leads to an iodo complex **3**, which was isolated in overall 46% yield after two steps. Both complexes were characterized by X-ray diffraction (Figure 1b, c), NMR, FT-IR, and UV-vis spectroscopies.[87-88] X-ray structures of **2** and **3** reveal a similar hexacoordinate Mn^{III} center with the Mn-Ar bond distances of 2.012(5) and 2.0323(18) Å, respectively. Thus, complexes **1-3** are rare examples of isolated, structurally characterized Mn^{III} monoaryl species.[89-92]

Since complex **1** was obtained via a formal 2e$^-$ oxidative addition to a Mn^I center, we decided to further examine if this transformation involves a free radical formation or occurs via a non-radical mechanism. When the reaction was carried out in the presence of (2,2,6,6-tetramethylpiperidin-1-yl)oxyl (TEMPO),[93] O$_2$[94] as radical traps or 9,10-dihydroanthracene[95-96] as an H-atom donor, no TEMPO adduct or anthracene could be detected in the reaction mixtures; the product of ligand hydrodebromination **^{t}BuN3CH** was also not detected, arguing against free Ar radical formation.[93, 95] The reaction in the presence of 1-hexene or 1-decene did not lead to the detection of brominated products by GC-MS analysis, which could be expected from formation of free Br radical or Br$_2$.[97-100] The role of UV light irradiation is likely to remove CO ligands, similar to the known photolabile Mn complexes.[101]

When isolated complex **1** was heated in toluene solution, no reductive elimination was observed up to up to 150 °C, with or without additives of PPh$_3$ or CO, showing that reductive elimination from Mn^{III} does not occur easily under these conditions.

Next we set out to investigate if Ar-Mn complexes in higher oxidation states will be accessible, which could induce more facile reductive elimination.[49, 62-64] The cyclic voltammetry of **1** in ^{n}Bu$_4$PF$_6$/CH$_3$CN revealed a quasireversible oxidation wave assigned tentatively as a Mn^{III}/Mn^{IV} oxidation at $E_{1/2}$ = 0.47 V vs. Fc$^+$/Fc (ΔE_p = 290 mV), followed by another irreversible oxidation at E_{pa} ≈ 1.12 V (Figure 2). The relatively low potential for the first oxidation suggests the 1e$^-$-oxidized product can be easily accessible by using conventional chemical oxidants.[102]

First, complex **1** was reacted with 1.1 equiv of NOBF$_4$ as an oxidant. NOBF$_4$ has a formal potential of 1.00 V and 0.87 V vs. Fc/Fc$^+$ in CH$_2$Cl$_2$ and MeCN, respectively. When the reaction was performed in CH$_2$Cl$_2$, the initial red-colored solution
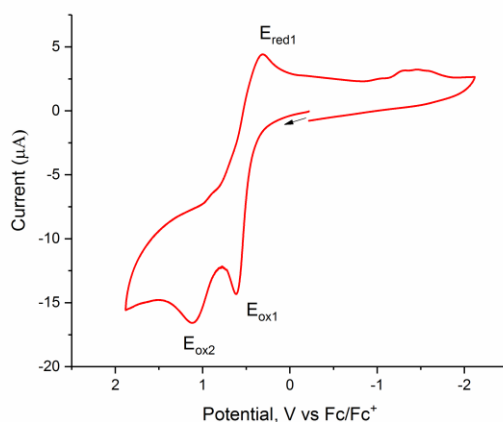

Figure 2. Cyclic voltammogram of **1** (2 mM) in 0.1 M ^{n}Bu$_4$NPF$_6$/MeCN at 25 °C (scan rate 50 mVs^{-1}; 1.6 mm Pt disk working electrode; the arrow indicates the initial scan direction). E_{ox1} = 0.611 V; E_{red1} = 0.321 V (quasirev.); ΔE_p = 290 mV; $E_{1/2}$ = 0.466 mV; E_{ox2} = 1.120 mV (irrev.).

gradually changed to yellow within 2 h, and in MeCN an instantaneous color change to yellow was observed. While the solution was NMR silent in the presence of Mn-containing product, HR-MS shows the peak with a characteristic isotope pattern at *m/z* 430.1836 corresponding to a metal-free [**^{t}BuN3CBr**+H]$^+$ (expected *m/z* 430.1852). Interestingly, when the reaction was performed using excess (2 equiv) of NOBF$_4$, crystals were obtained from MeCN showing a co-crystallized metal-free **^{t}BuN3CBr** together with [Mn(MeCN)$_6$]$^{2+}$, NO$^+$ and BF$_4^-$ counterions (Figure 1d). Although the charges and oxidation states of all components cannot be assigned unambiguously due to a disorder,[87] this structure additionally confirmed the formation of **^{t}BuN3CBr**. The presence of extra equivalents of NO$^+$ suggests that less than 2 equiv. of the oxidant might be necessary.

Indeed, when the reaction was performed in the presence of only 1.1 equiv of NOBF$_4$, complete disappearance of red-colored **1** was observed. The organic product was isolated by washing the CH$_2$Cl$_2$ solution with basic aqueous solution to remove Mn salts. NMR analysis shows that the crude CH$_2$Cl$_2$ solution contains free **^{t}BuN3CBr** in 84% yield based on integration vs. internal standard (Scheme 4, a).[87] Further purification via flash chromatography resulted in 65% isolated yield of pure **^{t}BuN3CBr** as an average of three trials. The side-product of the reaction was identified as the protonated ligand **^{t}BuN3CH** formed in *ca.* 16-17% yield, which likely results from protonation of the ligand by protic impurities in the oxidant or solvent. The formation of **^{t}BuN3CH** was also observed when the reaction was performed in CD$_2$Cl$_2$, CD$_3$CN or in CD$_2$Cl$_2$/toluene-d_8, indicating that **^{t}BuN3CH** is not formed by H-atom abstraction from the solvent or benzylic protons as expected for free Ar radical formation.[103]

In order to analyze the Mn-containing product, a sample of the reaction mixture, obtained by reacting **1** with 1.1 equiv of NOBF$_4$ in MeCN solution, was diluted with water and analyzed by EPR spectroscopy. The EPR spectrum at 298 K shows a characteristic sextet at g = 2.01 (A = 95 G) typical for Mn^{2+} salts showing hyperfine splitting from ^{55}Mn (I = 5/2) (Figure 3), almost identical to that for Mn(H$_2$O)$_6^{2+}$ obtained by dissolving MnSO$_4$ in water. Spin integration vs. standard solu-

Scheme 4. Oxidatively-induced reductive elimination of Ar-X bonds (X = Br, I, CN).
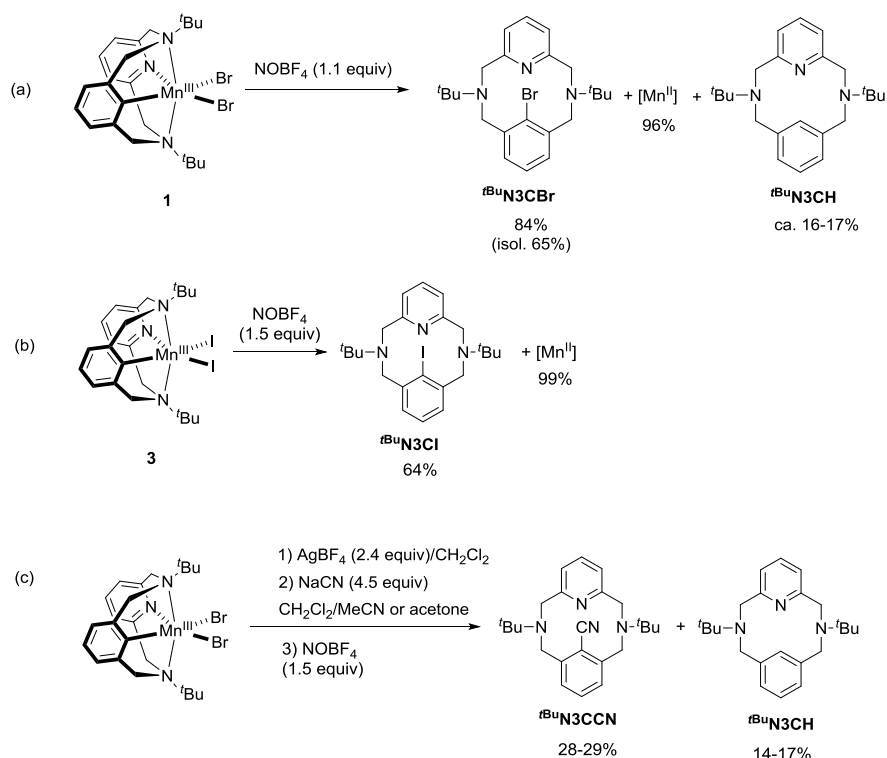
tion of $MnSO_4$ allowed us to estimate the yield as 96% from an average of two trials.[104]

Overall, quantitative formation of the Mn^{2+} salt and high isolated yield of ^{tBu}**N3CBr** implies that only 1.1 equiv of a one-electron oxidant, $NOBF_4$, was sufficient to complete Ar-Br reductive elimination. To our knowledge, this is the first example of the Ar-Br reductive elimination from a Mn monoaryl complex.

In order to examine if RE also occurs in the presence of other oxidants, we then performed oxidation of **1** using arylaminium radical "Magic Blue" $[N(4-BrC_6H_4)_3][SbCl_6]$ (1.1 equiv) ($E^{0'}$ = 0.70 V and 0.67 V vs. Fc/Fc$^+$ in CH_2Cl_2 and MeCN, respectively).[102] Although the reaction was slower, after 12 h, the organic product ^{tBu}**N3CBr** was obtained in 56% yield. Interestingly, even using H_2O_2 as an oxidant allowed us to obtain ^{tBu}**N3CBr** in 37% isolated yield. EPR analysis of the reaction mixtures revealed the presence of Mn^{2+} ion, with 70% and 62% yield of Mn^{2+} after oxidation with "Magic Blue" and H_2O_2, respectively.[87] Overall, these experiments indicate that the Ar-Br elimination is not specific to $NOBF_4$ and other oxidants may be used.

Next, to gain insight into the mechanism of this reaction, we performed the experiments in the presence of TEMPO or O_2 that could trap carbon-based radicals.[93-94] However, isolated yields were not affected significantly, and ^{tBu}**N3CBr** was obtained in 78-82% yields, while no TEMPO adduct was detected, indicating that free Ar radical formation does not have significant contribution.[93-94] The reaction in the presence of 1-decene did not show any products of bromination of 1-decene, suggesting that the reactivity does not involve either the metal bromide as the "surrogate" of the Br radical (or free Br radical) or Br_2.[97-100] We then attempted to detect proposed Mn^{IV} intermediates by a variable temperature UV-vis experiment at

-78 to 20 °C in propionitrile or acetonitrile, however, no persistent intermediates were detected.[87]

The frontier orbital analysis of the DFT-optimized structure for the proposed intermediate, complex **1**$^+$ (Scheme 1), shows that three singly-occupied molecular orbitals (SOMO's) have the character of d_{xy}, d_{xz} and d_{yz} orbitals at the metal (Figure 4), consistent with assignment of **1**$^+$ as a Mn^{IV} complex.[87] Although the possibility of ligand's non-innocence cannot be fully excluded, the use of ^{t}**BuN3C**$^-$ ligand and analogous chelating N-donor ligands in studying reductive elimination from first row transition metals (*e.g.* Cu^{III}, Ag^{III}, Ni^{III} species) is typically proposed to occur at the high-valent metal center without participation of the ligand.[35, 71-73, 76-78]

We then explored applicability of oxidatively-induced elimination to other types of Ar-X bonds. Unfortunately, the attempted synthesis of the corresponding chloro-complex (^{tBu}**N3C**)$Mn^{III}Cl_2$ failed to give the desired product by BF_4/Cl exchange. Complex **2** undergoes fast decomposition upon reaction with $NOBF_4$ to give ^{tBu}**N3CH** as a major identifiable product; no evidence was seen by ESI-MS or GC-MS for the formation of an Ar-F elimination product. Similarly, oxidation of **2** with $NOBF_4$ in the presence of MeOH yields ^{tBu}**N3CH** as a major product, while no methoxylation product could be detected. However, to our satisfaction, when iodo complex **3** was treated with 1.5 equiv. of $NOBF_4$, reductive elimination of Ar-I bond was also observed to give the expected product ^{tBu}**N3CI** in 64% yield determined by NMR integration vs. internal standard after extraction (Scheme 4, b), while ^{tBu}**N3CH** was not detected. The formation of a Mn^{II} species was also confirmed by EPR spectroscopy.[87]

Interestingly, one-pot Ar-CN elimination has also been achieved by reacting complex **1** with $AgBF_4$ to give **2**, which was further reacted with NaCN for 3 h, followed by oxidation
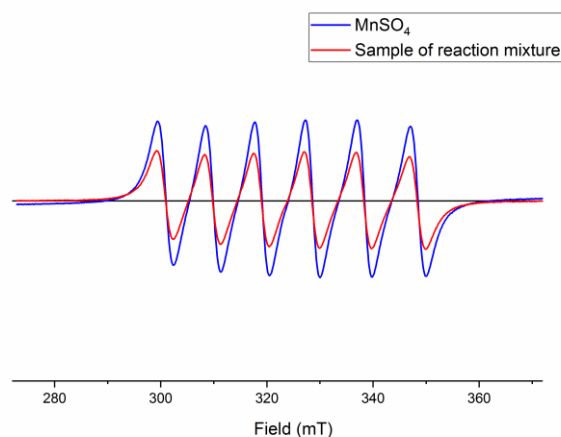
Figure 3. X-band EPR spectra of H_2O-diluted sample from oxidation of **1** with 1.1 equiv $NOBF_4$ (red) and reference sample of $MnSO_4$ in H_2O (blue) at 298 K.
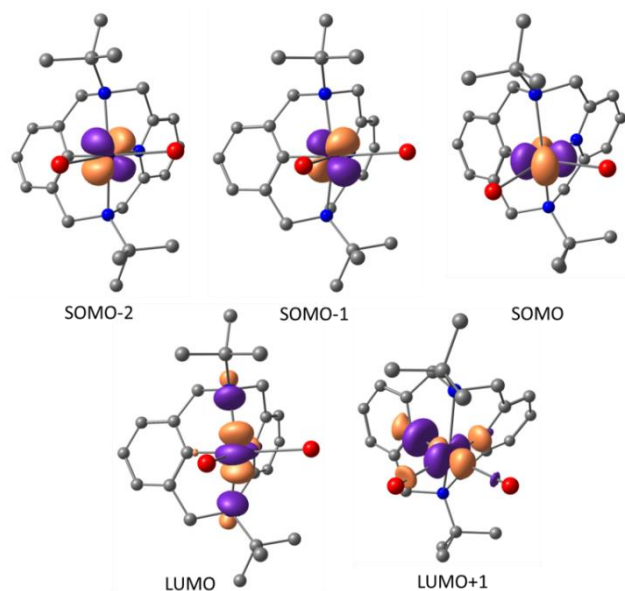

Figure 4. Kohn-Sham orbital plots for DFT-optimized complex **1**$^+$ (isovalue 0.07) (ROB3LYP/6-311++G(d,p)/LANL2DZ).

with $NOBF_4$. The expected ^{tBu}**N3CCN** product was obtained in 28-29% yield, with ^{tBu}**N3CH** as a side-product formed in 14-17% yield (Scheme 4, c).

Therefore, the oxidatively-induced RE reactivity is not limited to Ar-Br only and can be extended to other types of heteroatoms, which may potentially find wider applications in oxidatively-induced C-H and C-X bond functionalization. We will further investigate the possibility of chelation-assisted C-H and C-heteroatom bond activation by Mn^{II} or Mn^{III} species in the presence of an oxidant, which can potentially lead to the catalytic turnover for substrates containing directing groups.

SUMMARY AND CONCLUSION

In summary, we isolated rare, stable monoaryl Mn^{III} bromocomplexes obtained by oxidative addition of Ar-Br bond to a Mn^I precursor. While Mn^{III} complex **1** was stable, its one-electron oxidation induces facile reductive elimination of the

Ar-X (X = Br, I) bond and concurrent formation of a Mn^{II} species via a non-radical mechanism. Considering the wide use of Mn^I complexes for C-H bond activation leading to Ar-Mn complexes, observation of Ar-X bond-forming reductive elimination from Ar-Mn complexes opens up new possibilities for oxidative C-H functionalization. We were able to obtain isolated organometallic Mn^{III} species, which enable direct observation of both OA and RE of Ar-Br, demonstrating the importance of taking advantage of the large range of oxidation states available to the Mn metal center, with four oxidation states being necessary overall in the current transformation. We are currently investigating the possibility of other types of C-X and C-C bond reductive eliminations as well as catalytic C-H and C-X functionalization.

EXPERIMENTAL SECTION

General specifications. All manipulations unless stated otherwise were performed using Schlenk or glovebox techniques under dry argon atmosphere. Anhydrous solvents were dispensed from an MBRAUN solvent purification system and degassed prior to use. Anhydrous deuterated solvents were purchased from Eurisotop and stored over 4Å molecular sieves. All chemicals unless noted otherwise were purchased from major commercial suppliers (TCI, Sigma-Aldrich and NacalaiTesque) and used without purification.

Instrumentation. NMR spectra were measured on JEOL ECZ600R 600MHz, JEOL ECZ400S 400 MHz, Bruker Avance II 400 MHz and Bruker Avance III Neo 500 MHz (CryoProbe) spectrometers. Electrospray Ionization Mass Spectrometry (ESI-MS) measurements were performed on a Thermo Scientific ETD apparatus. Elemental analyses were performed using an Exeter Analytical CE440 instrument. FT-IR spectra were measured using Agilent Cary 630 with ATR module in an argon filled glovebox. The following abbreviations are used for describing FT-IR spectra: s (strong), m (medium), w (weak), br (broad). UV–vis absorbance spectra were collected using an Agilent Cary 60 instrument. EPR measurements were done on an X-band JEOL JES-X330 EPR spectrometer. The magnetic properties were measured using a 9T physical properties measurement system PPMS Dynacool from Quantum Design, equipped with the vibrating sample magnetometer (VSM) option, in a 2–300 K temperature range under a magnetic field of 10 000 Oe. For these measurements, samples were ground into powder and placed in plastic capsules. The Evans method measurements were performed in the coaxial NMR tube at 298 K; diamagnetic correction was applied.[105] Low temperature UV–vis measurements were performed using a fiber-optic immersion probe (Hellma, path length 2 mm). Cyclic voltammetry (CV) experiments were performed using ALS/CHI Electrochemical Analyzer 660E. Electrochemical grade ^{n}Bu$_4$NPF$_6$ was used as the supporting electrolyte. Electrochemical measurements were performed in an Ar-filled glove box. A Pt disk electrode (d = 1.6 mm) was used as the working electrode, and a Pt wire as the auxiliary electrode. The non-aqueous Ag-wire reference electrode assembly was filled with 0.01 M AgNO$_3$/0.1 M ^{n}Bu$_4$NClO$_4$/MeCN solution was used as a reference electrode and was calibrated against ferrocene (Fc). The potentials are reported in volts (V) at a scan rate of 50 mV s^{-1}.

X-ray structure determination details. The X-ray diffraction data for the single crystals were collected on a Rigaku XtaLab PRO instrument (κ-goniometer) with a PILATUS3 R 200K hybrid pixel array detector using Mo$K\alpha$ (0.71073 Å) or Cu$K\alpha$ (1.54184 Å) radiation monochromated by means of multilayer optics. The performance mode of MicroMax^{TM}-003 microfocus sealed X-ray tubes was 50 kV, 0.60 mA. The diffractometer was equipped with a Rigaku GN2 system for low temperature experiments. Suitable crystals of appropriate dimensions were mounted on loops in random orientations. Preliminary unit cell parameters were determined with three sets of a total of 10 narrow frame scans in the case of a Mo-source and six sets of a total of 10 narrow frame scans at two different 2θ positions in the case of a Cu-source. The data were collected according to recommended

strategies in an ω scan mode. Final cell constants were determined by global refinement of reflections from the complete data sets using the Lattice wizard module. Images were indexed and integrated with "smart" background evaluation using the *CrysAlis*[Pro] data reduction package (1.171.39.20a, Rigaku Oxford Diffraction, 2015). Analysis of the integrated data did not show any decay. Data were corrected for systematic errors and absorption using the ABSPACK module: Numerical absorption correction based on Gaussian integration over a multifaceted crystal model and empirical absorption correction based on spherical harmonics according to the point group symmetry using equivalent reflections. The GRAL module and the ASSIGN SPACEGROUP routine of the *WinGX* suite were used for analysis of systematic absences and space group determination.

The structures were solved by the direct methods using *SHELXT*-2018/2[106] and refined by the full-matrix least-squares on F^2 using *SHELXL*-2018/3,[107] which uses a model of atomic scattering based on spherical atoms. Calculations were mainly performed using the *WinGX*-2018.3 suite of programs[108] and *Olex*2.[109] Non-hydrogen atoms were refined anisotropically. The positions of the hydrogen atoms of methyl groups were found using rotating group refinement with idealized tetrahedral angles. The other hydrogen atoms were inserted at the calculated positions and refined as riding atoms. In the cases of **1** and **2**, a substitutional "N1/C1" disorder occurs. A positional disordering of tetrafluoroborate anions and acetonitrile ligands was observed for the crystals of "2(^{tBu}N3CBr) × [Mn(CH$_3$CN)$_6$]$^{2+}$ NO^{1+} 6(BF$_4$$^{1-}$)". The disorder was resolved using free variables and reasonable restraints on geometry and anisotropic displacement parameters. The unit cell of "2(^{tBu}N3CBr) × [Mn(CH$_3$CN)$_6$]$^{2+}$ NO^{1+} 6(BF$_4$$^{1-}$)" contains highly disordered nitrosonium ions and solvent molecules of hexane and/or acetonitrile, which were treated as a diffuse contribution to the overall scattering without specific atom positions by *PLATON*/SQUEEZE-200618.[110] Squeezed solvent info is not included in the formula and related items such as molecular weight and calculated density. The structure of **1** was treated as a 2-component inversion twin with the fractional volume contribution of 0.028(7) for the minor component. Complex **2** crystallizes as a dichloromethane solvate (1 : 1). In the case of "2(^{tBu}N3CBr) × [Mn(CH$_3$CN)$_6$]$^{2+}$ NO^{1+} 6(BF$_4$$^{1-}$)" , the complex cation Mn(NCCH$_3$)$_6$$^{2+}$ (through metal-center) bisected by glide plane in the space group *C2/c*, hence the asymmetric cell contains half of the cation (Z′ = 0.5). All the compounds studied have no unusual bond lengths and angles. The absolute structure of **1** was determined based on the Flack parameter.[111-112]

The crystal data, data collection and structure refinement details for the investigated crystals are summarized in Table S2 (Supp. Info). Molecular structures of the investigated complexes in the crystalline phase as well as accepted partial numbering are presented as ORTEP diagrams in Figures S50-S53 (Supp. Info). Selected bond lengths and angles are appended to the captions.

The crystallographic data for the investigated compounds have been deposited in the Cambridge Crystallographic Data Centre as supplementary publication numbers CCDC 1917063 (1), 1917064 (2), 1917065 (3), and 1917066 ("2(^{tBu}N3CBr) × [Mn(CH$_3$CN)$_6$]$^{2+}$ NO^{1+} 6(BF$_4$$^{1-}$)"). These data can be obtained free of charge via www.ccdc.cam.ac.uk/data_request/cif, or by emailing data_request@ccdc.cam.ac.uk, or by contacting The Cambridge Crystallographic Data Centre, 12 Union Road, Cambridge CB2 1EZ, UK; fax: +44 1223 336033.

Synthesis of (^{t}BuN3C)Mn^{III}Br$_2$ (1). 410 mg of ^{tBu}N3CBr ligand (0.952 mmol) and 261.4 mg of Mn(CO)$_5$Br (0.951 mmol) were combined in a flame dried Schlenk flask inside a glove box and 20 mL of dichloroethane was added to give a yellow suspension. The flask was taken outside the glove box and stirred in a water bath in front of a mercury lamp. The reaction vessel was subjected to vacuum for 1 second every hour, then stirred under static vacuum, and after 3 h, the reaction was then stirred under a static vacuum overnight. After 13 hours, the solution appeared wine-red and the entire solvent was evaporated under reduced pressure. The solid obtained was redissolved in a minimal amount of dichloromethane and filtered through celite. The filtrate obtained was evaporated under reduced pressure to yield a red solid which was washed three times with copious amounts

of ether (≈ 15 mL) and then dried to yield **1**. Deep red crystals were grown by vapor diffusion of ether into a dichloromethane solution of the complex (about 6 mL of DCM); yield of isolated product 310 mg (0.548 mmol), 58%. The product was recrystallized second time to give 260 mg of the crystalline product as large dark-red crystals (0.460 mmol).

UV-vis, λ, nm (ε, M^{-1}·cm^{-1}), CH$_2$Cl$_2$: 547 (560), 430 (620, sh), 383 (1720), 270 (10200).

μ$_{eff}$ = 4.98 μB (298 K, Evans method, CD$_2$Cl$_2$).

FT-IR (ATR, solid, cm^{-1}): ν 3049 (w), 2972 (w), 2008 (w), 1926 (w), 1598 (w), 1575 (w), 1457 (w), 1430 (w), 1267 (s), 1194 (w), 849 (w), 731 (s), 701 (m).

^{1}H NMR (CD$_2$Cl$_2$, 400 MHz, 25 °C), δ: 47.80 (br), 36.55 (br), 23.73 (br), 11.38, 3.73, 3.42, 1.29, 1.14, 0.87, 0.08, -20.49 (br), -105.21 (br), -154.97 (br).

ESI-HRMS in CH$_3$CN (*m/z*): calculated for [C$_{23}$H$_{32}$BrN$_3$Mn]$^+$, ([M-Br]$^+$, *z* = 1): 484.1155; Found: 484.1149.

Anal. Calcd. for Mn$_1$C$_{23}$H$_{32}$Br$_2$N$_3$: C, 49.02; H, 5.72; N, 7.46. Found: C, 49.01; H, 5.75; N, 7.47.

Synthesis of (^{tBu}N3C)Mn^{III}(BF$_4$)$_2$ (2). 30.0 mg (0.0531 mmol) of **1** was dissolved in 2 mL of dichloromethane and 20.7 mg (0.106 mmol) of AgBF$_4$was added and stirred for 3 hours in the dark. The AgBr salt was filtered off to give a yellow-colored filtrate containing complex **2**. The solution was used immediately for the next step or for reactivity studies. Compound **2** was stable in solution at RT: no changes were observed in the UV/vis spectrum of a 0.36 mM solution of **2** stored in the dark under Ar atmosphere for at least 24 h. Upon removal of solvent and drying under vacuum, the compound gradually decomposed into a black unidentifiable compound. Thus, complex **2** was used as a freshly prepared solution without isolation and stored in the dark and could not be isolated in a pure form as a solid.

Pink crystals of **2** were grown by vapor diffusion with hexane of a dichloromethane solution in a freezer at -20 °C.

UV-vis, λ, nm (ε, M^{-1}·cm^{-1}), CH$_2$Cl$_2$: 560 (440), 440 (305, sh), 352 (2200), 262 (7700).

FT-IR (ATR, dichloromethane solution, cm^{-1}): ν 3513 (m), 2029 (w), 1625 (w), 1458 (w), 1445 (w), 1389 (w), 1174 (w), 1007 (s, br).

^{1}H NMR (CD$_2$Cl$_2$, 400 MHz, 25 °C), δ: 45.68 (br), 24.12 (br), 11.10 (br), 3.41, 1.72, 1.41, 1.23, 1.13, -22.21 (br), -113.00 (br), -138.65 (br).

ESI-HRMS fails to show the expected peaks, presumably due to labile nature of BF$_4$ ligands and coordinating solvents used for analysis.

Elemental Analyses could not be performed because of instability of **2** in solid state.

Synthesis of (^{tBu}N3C)Mn^{III}I$_2$ (3). Step 1: 71.5 mg (0.1265 mmol, 1.0 equiv.) of **1** was dissolved in 5 mL of dichloromethane and 59.1 mg (0.3036 mmol, 2.4 equiv.) of AgBF$_4$ was added and stirred for 3 hours in the dark. The AgBr salt was filtered off through a pad of celite to give a yellow-colored filtrate containing complex **2**. The solution was used immediately for the next step.

Step 2: To the above solution, 57.0 mg (0.3795 mmol, 3.0 equiv) of sodium iodide in acetone (2.5 mL) was added. The resulting mixture was stirred for 2.5 hours and filtered through a pad of celite. The filtrate obtained was evaporated under reduced pressure to yield a red solid which was dried to yield **3**. Deep red crystals were grown from by vapor diffusion of ether into a dichloromethane solution of the complex. The desired complex **3** was obtained in 46% yield (38 mg) after two recrystallizations.

Complex **3** can also be generated through a reaction of *in situ* prepared **2** with 2 equiv of ^{n}Bu$_4$NI, however, it cannot be completely purified from ^{n}Bu$_4$N$^+$ salts due to their high solubility in organic solvents.

UV-vis, λ, nm (ε, M^{-1}·cm^{-1}), CH$_2$Cl$_2$: 558 (1500), 450 (1500, sh), 380 (4400, sh), 311 (8000).

FT-IR (ATR, solid, cm^{-1}): ν 2968 (m), 2908 (w), 1602 (w), 1568 (w), 1462 (m), 1423 (m), 1372 (m), 1189 (s), 997 (m), 903 (m), 843 (m), 766 (m).

^{1}H NMR (CD$_2$Cl$_2$, 400 MHz, 25 °C), δ: 45.1 (br), 37.3 (br) 24.3, 10.8 (br), 3.44, 1.17, -20.7, -22.9, -111.3 (br), -153.6 (br).

μ_{eff} = 5.33 µB (298 K, Evans method, CD_2Cl_2).

ESI-HRMS in CH_3CN failed to give the signals expected from [M-I]$^+$ ion.

Anal. Calcd. for $MnC_{23}H_{32}I_2N_3$: C, 41.88; H, 4.89; N, 6.37. Found: C, 43.35; H, 4.82; N, 6.58.

Oxidation of 1 with NOBF$_4$. 56.3 mg (0.1 mmol) of **1** was weighed out in a scintillation vial inside a glove box and 5 mL of dichloromethane was added. To the red solution, 12.2 mg (0.11 mmol) of NOBF$_4$ was added in one portion and the mixture was allowed to stir for 2 hours over which time period the color of the solution gradually changed to yellow and the reaction was stopped. The analogous procedure was used for reaction with MeCN leading to immediate color changes to yellow.

ESI-(HR)MS of the crude reaction mixture shows the presence of the signal expected for **^{tBu}N3CBr** product (as [M+H]$^+$) having a characteristic isotopic pattern.

From MeCN solution (first most intense peak): *m/z* 430.1837 (expected [M+H]$^+$, $C_{23}H_{33}N_3Br$, *m/z* 430.1852)

From CH_2Cl_2 solution (first most intense peak): *m/z* 430.1836 (expected [M+H]$^+$, $C_{23}H_{33}N_3Br$, *m/z* 430.1852).

The products were further characterized and isolated as described below.

Oxidation of 1 by 2 equiv of NOBF$_4$ in MeCN and crystallization of the co-crystal of ^{tBu}N3CBr with Mn(MeCN)$_6$$^{2+}$ and NO$^+$ and BF$_4$$^-$ counterions. 56.3 mg (0.1 mmol) of **1** was weighed out in a scintillation vial inside a glove box and 5 mL of acetonitrile was added. To the red solution, 1.1 equiv (for ESI-MS measurements) or 2 equiv (for crystallization) of NOBF$_4$ was added in one portion and the mixture was allowed to stir for 2 hours and analyzed by ESI-MS. The resulting yellow solution was concentrated to *ca.* 2 mL, filtered through a small pad of celite and crystals of the adduct were grown by vapor diffusion of ether into the filtrate.

Isolation of ^{tBu}N3CBr product after oxidation. 56.3 mg (0.1 mmol) of **1** was weighed out in a scintillation vial inside a glove box and 5 mL of dichloromethane was added. To the red solution, 12.2 mg (0.11 mmol) of NOBF$_4$ was added in one portion and the mixture was allowed to stir for 2 hours over which time period the color of the solution gradually changed to yellow and the reaction was stopped. The solvent was then completely removed under vacuum and the yellow solid was dried completely. The vial was then taken out of the glove box and then a 5 mL saturated solution of K_2CO_3 was added to it and vigorously stirred for 30 minutes. Initially some effervescence is seen and gradually a dark brown precipitate appears. The aqueous solution was extracted with dichloromethane, filtered and then dried over anhydrous MgSO$_4$. The dichloromethane was completely evaporated by a rotavapor and the solid left behind was identified to be **^{tBu}N3CBr**. NMR yield was confirmed by adding 1,3,5-trimethoxybenzene (0.33 mmol) to the CDCl$_3$ solution. Analytically pure **^{tBu}N3CBr** could be isolated by a short flash column chromatography in 3:97 methanol: dichloromethane mixture. *In situ* yield (before chromatography) was found to be 84% based upon internal standard, whereas isolated yields were averaged to be 65% based on average three runs.

Isolation of **^{tBu}N3CBr** was performed after reaction in CH_2Cl_2 solution, since attempted isolation from CH_3CN even after evaporation of the solvent leads to partial transferring of the paramagnetic species (presumably solvated Mn^{2+} ion) into the organic layer even after treatment with a base, leading to broadening of NMR spectra.

^{1}H NMR (400 MHz, CDCl$_3$), δ: 7.13 (t, *J* = 7.6 Hz, 1H, ArH), 6.79 (d, *J* = 7.5 Hz, 2H, ArH), 6.74 (d, *J* = 7.6 Hz, 2H, ArH), 6.60 (t, *J* = 7.4 Hz, 1H, ArH), 4.19-4.10 (m, 4H, two CH$_2$ groups), 4.04 (d, *J* = 12.8 Hz, 2H, CH$_2$), 3.57 (d, *J* = 13.3 Hz, 2H, CH$_2$), 1.32 (s, 18H, tBu).

^{13}C NMR (101 MHz, CDCl$_3$), δ: 160.05, 138.88, 135.04, 131.54, 131.08, 125.69, 121.38, 56.78, 55.94, 54.47, 27.85.

ESI-(HR)MS (first most intense peak): *m/z* 430.1837 (calcd. [M+H]$^+$, $C_{23}H_{33}N_3Br$, *m/z* 430.1852).

Quantitative determination of a Mn^{2+} product by spin integration. Standard 10.0 mM MnSO$_4$ solution in water was prepared for comparison of spin integration values. Measurements were performed in quartz precision capillary tubes (50 µL) at RT; microwave frequency 9114 MHz.

14.1 mg (25 µmol) of **1** was dissolved in 4 mL acetonitrile and 3.2 mg (1.1 equiv) of NOBF$_4$ was added and stirred for 1 hour. 1000 µL aliquot of this solution was taken and diluted to 10 mL by addition of 9 mL water in a volumetric flask to give a final solution with a final expected concentration of Mn species of 0.625 mM.

EPR measurements were performed at RT in the quartz thin capillary tubes. Spin integration was compared for the reaction mixture and the standard MnSO$_4$ solution. The measurements were performed two times and average of two runs was used. The concentration of Mn^{2+} in the final solution was calculated as 0.601 mM corresponding to the yield of 96% as an average of two trials.

The sextet corresponding to Mn^{2+} species obtained from the reaction mixture was observed at g = 2.01 and shows hyperfine splitting to ^{55}Mn (I = 5/2; A = 95 G). Identical signal was obtained by dissolving MnSO$_4$ is water (g = 2.01, A = 95 G).

Oxidation of 3 with NOBF$_4$. A 20 mL vial was charged with compound 3 (23.0 mg, 0.0349 mmol, 1.0 equiv.), NOBF$_4$ (6.1 mg, 0.0524 mmol, 1.5 equiv.) and DCM (3 mL). The mixture was allowed to stir for 3 hours in glove box, over which time period the color of the solution gradually changed to yellow and the reaction was stopped (about 3 h). The vial was then taken out of the glove box and then a 4 mL saturated solution of K_2CO_3 was added to it and vigorously stirred for 30 minutes. The aqueous solution was extracted with EtOAc (3 x 30 mL), filtered and then dried over anhydrous Na$_2$SO$_4$. The EtOAc was completely evaporated by a rotary evaporator. 1,3,5-Trimethoxybenzene (5.9 mg, 0.0349 mmol, 1.0 equiv.) was added as an internal standard. The yield of the product **^{tBu}N3CI** was 64%.

ESI-MS analysis shows that only the peak corresponding to protonated **^{t}BuN3CI** could be detected, while no peaks that could correspond to **^{t}BuN3CBr** or **^{t}BuN3CH** were present.

The **^{tBu}N3CI** product was further isolated and purified by column chromatography (eluting with 5% MeOH – DCM initially, grading to 10% MeOH – DCM, linear gradient) and identified by ^{1}H, ^{13}C, 2D NMR and HRMS.

When complex 3 is generated in situ using ^{n}BuNI instead of NaI and further oxidized by NOBF$_4$, formation of **^{t}BuN3CI** is also observed by NMR and ESI-MS, however, the reaction is generally less selective and the pure product could not be completely separated from ^{n}BuN$^+$ salts.

^{1}H NMR (500 MHz, benzene-d$_6$) δ 6.95 (t, *J* = 7.6 Hz, 1H, CH$_{ar}$), 6.81 (d, *J* = 7.3 Hz, 2H, CH$_{ar}$), 6.69 (d, *J* = 7.6 Hz, 2H, CH$_{ar}$), 6.59 (t, *J* = 7.4 Hz, 1H, CH$_{ar}$), 4.31 (d, *J* = 12.6 Hz, 2H, CH$_2$), 4.10 (d, *J* = 12.6 Hz, 2H, CH$_2$), 4.01 (d, *J* = 13.7 Hz, 2H, CH$_2$), 3.90 (d, *J* = 13.7 Hz, 2H, CH$_2$), 1.13 (s, 18H, ^{t}Bu).

^{13}C NMR (126 MHz, benzene-d$_6$) δ 160.5 (C$_{quat}$), 142.0 (C$_{quat}$), 134.7 (CH$_{ar}$), 131.6 (CH$_{ar}$), 126.6 (CH$_{ar}$), 121.1 (CH$_{ar}$), 114.8 (C$_{quat}$), 60.5 (CH$_2$), 57.0 (CH$_2$), 55.7 (*C*(CH$_3$)$_3$), 27.7 (C(*C*H$_3$)$_3$).

ESI-(HR)MS: *m/z* 478.1717 (calcd. M*H$^+$, $C_{23}H_{33}N_3I$, *m/z* 478.1714).

One-pot oxidatively induced Ar-CN elimination. 28.3 mg (0.05 mmol, 1.0 equiv) of **1** was dissolved in 3 mL of dichloromethane and 23.4 mg (0.12 mmol, 2.4 equiv) of AgBF$_4$ was added and stirred for 3 hours in the dark. The AgBr salt was filtered off through a pad of celite to give a yellow-colored filtrate containing complex **2**. To the above solution, 11.0 mg (0.2245 mmol, 4.5 equiv) of sodium cyanide in acetonitrile (2.0 mL) was added. The resulting mixture was stirred for 3 hours. 8.8 mg (0.075 mmol) of NOBF$_4$ was added in one portion and the mixture was allowed to stir for 2.5 hours over which time period the color of the solution gradually changed to yellow and the reaction was stopped. The vial was then taken out of the glove box and then a 5 mL saturated solution of K_2CO_3 was added to it and vigorously stirred for 30 minutes. The aqueous solution was extracted with dichloromethane, filtered and then dried over anhydrous Na$_2$SO$_4$. The dichloromethane was completely evaporated by a rotavapor and the residue was purified by flash-column chromatography on silica gel (DCM/MeOH, 20:1 ~ 10:1) to provide the final products **^{tBu}N3CCN** (5.5 mg, 29%) and **^{tBu}N3CH** (3.0 mg, 17%).

The analogous procedure using acetone instead of acetonitrile yields similar yields of products, **^{tBu}N3CCN** (5.2 mg, 28%) and **^{tBu}N3CH** (2.5 mg, 15%).

^{1}H NMR (400 MHz, benzene-d_6) δ 6.87 (t, J = 7.6 Hz, 1H, CH$_{ar}$), 6.78 (d, J = 7.6 Hz, 2H, CH$_{ar}$), 6.67 (t, J = 7.6 Hz, 1H, CH$_{ar}$), 6.59 (d, J = 7.6 Hz, 2H, CH$_{ar}$), 4.17 (d, J = 12.7 Hz, 2H, CH$_2$), 4.01 (br m, 2H, CH$_2$), 3.86 (d, J = 13.6 Hz, 4H, CH$_2$), 1.08 (s, 18H, ^{t}Bu).

^{13}C NMR (101 MHz, benzene-d_6) δ 160.5 (C$_{quat}$), 143.8 (C$_{quat}$), 135.3 (CH$_{ar}$), 130.7 (CH$_{ar}$), 130.5 (CH$_{ar}$), 121.6 (CH$_{ar}$), 118.8 (C$_{quat}$), 58.3 (CH$_2$), 56.2 (C(CH$_3$)$_3$), 54.5 (CH$_2$), 28.0 (C(CH$_3$)$_3$).

ESI-(HR)MS: m/z 377.2693 (calcd. [M+H]$^+$, C$_{24}$H$_{32}$N$_4$, m/z 377.2700).

ASSOCIATED CONTENT

Supporting Information

The Supporting Information is available free of charge on the ACS Publications website.

Experimental details, characterization data as well as X-ray structures (CCDC 1917063-1917066), computational details (PDF)

Cartesian coordinates of geometry-optimized structures (XYZ)

AUTHOR INFORMATION

Corresponding Author

* juliak@oist.jp
Author contributions
§These authors contributed equally.

ORCID

Abir Sarbajna: 0000-0003-2478-5044

Yu-Tao He: 0000-0001-5280-8448

S. M. Wahidur Rahaman: 0000-0003-4922-5297

Ayumu Karimata: 0000-0003-0323-2256

Eugene Khaskin: 0000-0003-1790-704X

Sébastien Lapointe: 0000-0003-3190-3803

Robert R. Fayzullin: 0000-0002-3740-9833

Julia R. Khusnutdinova: 0000-0002-5911-4382

Notes
The authors declare no competing financial interests.

REFERENCES

1.	Hartwig, J. F. *Organotransition Metal Chemistry: From Bonding to Catalysis*. University Science Books: 2010.

2.	Crabtree, R. H. *The Organometallic Chemistry of the Transition Metals*. Wiley: 2005.

3.	Labinger, J. A. Tutorial on Oxidative Addition. *Organometallics* **2015,** *34*, 4784-4795.

4.	Rej, S.; Chatani, N. Rhodium-Catalyzed C(sp^2)- or C(sp^3)-H Bond Functionalization Assisted by Removable Directing Groups. *Angew. Chem. Int. Ed.* **2019,** *58*, 8304-8329.

5.	He, J.; Wasa, M.; Chan, K. S. L.; Shao, Q.; Yu, J.-Q. Palladium-Catalyzed Transformations of Alkyl C-H Bonds. *Chem. Rev.* **2017,** *117*, 8754-8786.

6.	Engle, K. M.; Mei, T.-S.; Wasa, M.; Yu, J.-Q. Weak Coordination as a Powerful Means for Developing Broadly Useful C-H Functionalization Reactions. *Acc. Chem. Res.* **2012,** *45*, 788-802.

7.	Lyons, T. W.; Sanford, M. S. Palladium-Catalyzed Ligand-Directed C-H Functionalization Reactions. *Chem. Rev.* **2010,** *110*, 1147-1169.

8.	Oloo, W.; Zavalij, P. Y.; Zhang, J.; Khaskin, E.; Vedernikov, A. N. Preparation and C-X Reductive Elimination Reactivity of Monoaryl Pd^{IV}-X Complexes in Water (X = OH, OH$_2$, Cl, Br). *J. Am. Chem. Soc.* **2010,** *132*, 14400-14402.

9.	Zeineddine, A.; Estevez, L.; Mallet-Ladeira, S.; Miqueu, K.; Amgoune, A.; Bourissou, D. Rational development of catalytic Au(I)/Au(III) arylation involving mild oxidative addition of aryl halides. *Nat. Commun.* **2017,** *8*, 1-8.

10.	Powers, D. C.; Benitez, D.; Tkatchouk, E.; Goddard, W. A., III; Ritter, T. Bimetallic reductive elimination from dinuclear Pd(III) complexes. *J. Am. Chem. Soc.* **2010,** *132*, 14092-14103.

11.	Roy, A. H.; Hartwig, J. F. Directly Observed Reductive Elimination of Aryl Halides from Monomeric Arylpalladium(II) Halide Complexes. *J. Am. Chem. Soc.* **2003,** *125*, 13944-13945.

12.	Winston Matthew, S.; Wolf William, J.; Toste, F. D. Halide-Dependent Mechanisms of Reductive Elimination from Gold(III). *J. Am. Chem. Soc.* **2015,** *137*, 7921-8.

13.	Brown, M. P.; Puddephatt, R. J.; Upton, C. E. E. Mechanism of reductive elimination of ethane from some halogenotrimethylbis(tertiary phosphine)platinum(IV) complexes. *J. Chem. Soc., Dalton Trans.* **1974**, 2457-2465.

14.	Williams, B. S.; Holland, A. W.; Goldberg, K. I. Direct Observation of C−O Reductive Elimination from Pt(IV). *J. Am. Chem. Soc.* **1999,** *121*, 252-253.

15.	Yahav-Levi, A.; Goldberg, I.; Vigalok, A. Aryl-Halide versus Aryl−Aryl Reductive Elimination in Pt(IV)−Phosphine Complexes. *J. Am. Chem. Soc.* **2006,** *128*, 8710-8711.

16.	Vigalok, A. Electrophilic Halogenation-Reductive Elimination Chemistry of Organopalladium and -Platinum Complexes. *Acc. Chem. Res.* **2015,** *48*, 238-247.

17.	Gandeepan, P.; Müller, T.; Zell, D.; Cera, G.; Warratz, S.; Ackermann, L. 3d Transition Metals for C–H Activation. *Chem. Rev.* **2019,** *119*, 2192-2452.

18.	Liu, W.; Ackermann, L. Manganese-Catalyzed C–H Activation. *ACS Catal.* **2016,** *6*, 3743-3752.

19.	Liu, W.; Zell, D.; John, M.; Ackermann, L. Manganese-catalyzed synthesis of *cis*-β-amino acid esters through organometallic C-H activation of ketimines. *Angew. Chem. Int. Ed.* **2015,** *54*, 4092-4096.

20.	Liu, W.; Bang, J.; Zhang, Y.; Ackermann, L. Manganese(I)-Catalyzed C-H Aminocarbonylation of Heteroarenes. *Angew. Chem. Int. Ed.* **2015,** *54*, 14137-14140.

21.	Shi, L.; Zhong, X.; She, H.; Lei, Z.; Li, F. Manganese catalyzed C-H functionalization of indoles with alkynes to synthesize bis/trisubstituted indolylalkenes and carbazoles: the acid is the key to control selectivity. *Chem. Commun.* **2015,** *51*, 7136-7139.

22.	Kuninobu, Y.; Nishina, Y.; Takeuchi, T.; Takai, K. Manganese-catalyzed insertion of aldehydes into a C-H bond. *Angew. Chem. Int. Ed.* **2007,** *46*, 6518-6520.

23.	Zhou, B.; Hu, Y.; Wang, C. Manganese-Catalyzed Direct Nucleophilic C(sp^2)-H Addition to Aldehydes and Nitriles. *Angew. Chem. Int. Ed.* **2015,** *54*, 13659-13663.

24.	Zhou, B.; Chen, H.; Wang, C. Mn-Catalyzed Aromatic C-H Alkenylation with Terminal Alkynes. *J. Am. Chem. Soc.* **2013,** *135*, 1264-1267.

25.	Carney, J. R.; Dillon, B. R.; Thomas, S. P. Recent Advances of Manganese Catalysis for Organic Synthesis. *Eur. J. Org. Chem.* **2016,** *2016*, 3912-3929.

26.	Cahiez, G.; Duplais, C.; Buendia, J. Chemistry of Organomanganese(II) Compounds. *Chem. Rev.* **2009,** *109*, 1434-1476.

27.	Fürstner, A. Iron Catalysis in Organic Synthesis: A Critical Assessment of What It Takes To Make This Base Metal a Multitasking Champion. *ACS Cent. Sci.* **2016,** *2*, 778-789.

28.	Chirik, P. J.; Wieghardt, K. Radical Ligands Confer Nobility on Base-Metal Catalysts. *Science* **2010,** *327*, 794.

29.   Abel, E. W.; Casey, C. P.; Wilkinson, G. *Manganese Group*. Elsevier Science: 1995.

30.   Layfield, R. A. Manganese(II): the black sheep of the organometallic family. *Chem. Soc. Rev.* **2008**, *37*, 1098-1107.

31.   Fürstner, A.; Martin, R.; Krause, H.; Seidel, G.; Goddard, R.; Lehmann, C. W. Preparation, Structure, and Reactivity of Nonstabilized Organoiron Compounds. Implications for Iron-Catalyzed Cross Coupling Reactions. *J. Am. Chem. Soc.* **2008**, *130*, 8773-8787.

32.   Neidig, M. L.; Carpenter, S. H.; Curran, D. J.; DeMuth, J. C.; Fleischauer, V. E.; Iannuzzi, T. E.; Neate, P. G. N.; Sears, J. D.; Wolford, N. J. Development and Evolution of Mechanistic Understanding in Iron-Catalyzed Cross-Coupling. *Acc. Chem. Res.* **2019**, *52*, 140-150.

33.   Sears, J. D.; Neate, P. G. N.; Neidig, M. L. Intermediates and Mechanism in Iron-Catalyzed Cross-Coupling. *J. Am. Chem. Soc.* **2018**, *140*, 11872-11883.

34.   Zheng, B.; Tang, F.; Luo, J.; Schultz, J. W.; Rath, N. P.; Mirica, L. M. Organometallic Nickel(III) Complexes Relevant to Cross-Coupling and Carbon–Heteroatom Bond Formation Reactions. *J. Am. Chem. Soc.* **2014**, *136*, 6499-6504.

35.   Zhou, W.; Schultz, J. W.; Rath, N. P.; Mirica, L. M. Aromatic Methoxylation and Hydroxylation by Organometallic High-Valent Nickel Complexes. *J. Am. Chem. Soc.* **2015**, *137*, 7604-7607.

36.   Schultz, J. W.; Fuchigami, K.; Zheng, B.; Rath, N. P.; Mirica, L. M. Isolated Organometallic Nickel(III) and Nickel(IV) Complexes Relevant to Carbon–Carbon Bond Formation Reactions. *J. Am. Chem. Soc.* **2016**, *138*, 12928-12934.

37.   Zhou, W.; Watson, M. B.; Zheng, S.; Rath, N. P.; Mirica, L. M. Ligand effects on the properties of Ni(III) complexes: aerobically-induced aromatic cyanation at room temperature. *Dalton Trans.* **2016**, *45*, 15886-15893.

38.   Lefèvre, G.; Jutand, A. Activation of Aryl and Heteroaryl Halides by an Iron(I) Complex Generated in the Reduction of [Fe(acac)₃] by PhMgBr: Electron Transfer versus Oxidative Addition. *Chem. Eur. J.* **2014**, *20*, 4796-4805.

39.   Lefèvre, G.; Taillefer, M.; Adamo, C.; Ciofini, I.; Jutand, A. First Evidence of the Oxidative Addition of Fe⁰(N,N)₂ to Aryl Halides: This Precondition Is Not a Guarantee of Efficient Iron-Catalysed C-N Cross-Coupling Reactions. *Eur. J. Org. Chem.* **2011**, *2011*, 3768-3780.

40.   Carpenter, S. H.; Baker, T. M.; Muñoz, S. B.; Brennessel, W. W.; Neidig, M. L. Multinuclear iron–phenyl species in reactions of simple iron salts with PhMgBr: identification of Fe₄(μ-Ph)₆(THF)₄ as a key reactive species for cross-coupling catalysis. *Chem. Sci.* **2018**, *9*, 7931-7939.

41.   Smith, A. L.; Hardcastle, K. I.; Soper, J. D. Redox-Active Ligand-Mediated Oxidative Addition and Reductive Elimination at Square Planar Cobalt(III): Multielectron Reactions for Cross-Coupling. *J. Am. Chem. Soc.* **2010**, *132*, 14358-14360.

42.   Rummelt, S. M.; Zhong, H.; Leonard, N. G.; Semproni, S. P.; Chirik, P. J. Oxidative Addition of Dihydrogen, Boron Compounds, and Aryl Halides to a Cobalt(I) Cation Supported by a Strong-Field Pincer Ligand. *Organometallics* **2019**, *38*, 1081-1090.

43.   Font, M.; Parella, T.; Costas, M.; Ribas, X. Catalytic C-S, C-Se, and C-P Cross-Coupling Reactions Mediated by a Cuᴵ/Cuᴵᴵᴵ Redox Cycle. *Organometallics* **2012**, *31*, 7976-7982.

44.   Casitas, A.; Canta, M.; Sola, M.; Costas, M.; Ribas, X. Nucleophilic Aryl Fluorination and Aryl Halide Exchange Mediated by a Cuᴵ/Cuᴵᴵᴵ Catalytic Cycle. *J. Am. Chem. Soc.* **2011**, *133*, 19386-19392.

45.   Fier, P. S.; Luo, J.; Hartwig, J. F. Copper-Mediated Fluorination of Arylboronate Esters. Identification of a Copper(III) Fluoride Complex. *J. Am. Chem. Soc.* **2013**, *135*, 2552-2559.

46.   Fier, P. S.; Hartwig, J. F. Copper-Mediated Fluorination of Aryl Iodides. *J. Am. Chem. Soc.* **2012**, *134*, 10795-10798.

47.   Lee, H.; Boergel, J.; Ritter, T. Carbon-fluorine reductive elimination from nickel(III) complexes. *Angew. Chem. Int. Ed.* **2017**, *56*, 6966-6969.

48.   Lee, E.; Hooker, J. M.; Ritter, T. Nickel-Mediated Oxidative Fluorination for PET with Aqueous [18F] Fluoride. *J. Am. Chem. Soc.* **2012**, *134*, 17456-17458.

49.   Higgs, A. T.; Zinn, P. J.; Simmons, S. J.; Sanford, M. S. Oxidatively Induced Carbon−Halogen Bond-Forming Reactions at Nickel. *Organometallics* **2009**, *28*, 6142-6144.

50.   Meucci, E. A.; Ariafard, A.; Canty, A. J.; Kampf, J. W.; Sanford, M. S. Aryl-Fluoride Bond-Forming Reductive Elimination from Nickel(IV) Centers. *J. Am. Chem. Soc.* **2019**, *141*, 13261-13267.

51.   Camasso, N. M.; Sanford, M. S. Design, synthesis, and carbon-heteroatom coupling reactions of organometallic nickel(IV) complexes. *Science* **2015**, *347*, 1218-1220.

52.   Hammarback, L. A.; Robinson, A.; Lynam, J. M.; Fairlamb, I. J. S. Mechanistic Insight into Catalytic Redox-Neutral C–H Bond Activation Involving Manganese(I) Carbonyls: Catalyst Activation, Turnover, and Deactivation Pathways Reveal an Intricate Network of Steps. *J. Am. Chem. Soc.* **2019**, *141*, 2316-2328.

53.   Sato, T.; Yoshida, T.; Al Mamari, H. H.; Ilies, L.; Nakamura, E. Manganese-Catalyzed Directed Methylation of C(sp²)-H Bonds at 25 °C with High Catalytic Turnover. *Org. Lett.* **2017**, *19*, 5458-5461.

54.   Zhu, C.; Oliveira, J. C. A.; Shen, Z.; Huang, H.; Ackermann, L. Manganese(II/III/I)-Catalyzed C–H Arylations in Continuous Flow. *ACS Catal.* **2018**, *8*, 4402-4407.

55.   Cahiez, G.; Moyeux, A.; Buendia, J.; Duplais, C. Manganese- or Iron-Catalyzed Homocoupling of Grignard Reagents Using Atmospheric Oxygen as an Oxidant. *J. Am. Chem. Soc.* **2007**, *129*, 13788-13789.

56.   Dakarapu, R.; Falck, J. R. Stereospecific Stille Cross-Couplings Using Mn(II)Cl₂. *J. Org. Chem.* **2018**, *83*, 1241-1251.

57.   Liu, W.; Groves, J. T. Manganese Catalyzed C–H Halogenation. *Acc. Chem. Res.* **2015**, *48*, 1727-1735.

58.   Huang, X.; Bergsten, T. M.; Groves, J. T. Manganese-Catalyzed Late-Stage Aliphatic C–H Azidation. *J. Am. Chem. Soc.* **2015**, *137*, 5300-5303.

59.   Liu, W.; Groves, J. T. Manganese-Catalyzed Oxidative Benzylic C–H Fluorination by Fluoride Ions. *Angew. Chem. Int. Ed.* **2013**, *52*, 6024-6027.

60.   Liu, W.; Huang, X.; Cheng, M.-J.; Nielsen, R. J.; Goddard, W. A.; Groves, J. T. Oxidative Aliphatic C-H Fluorination with Fluoride Ion Catalyzed by a Manganese Porphyrin. *Science* **2012**, *337*, 1322.

61.   Liu, W.; Groves, J. T. Manganese Porphyrins Catalyze Selective C−H Bond Halogenations. *J. Am. Chem. Soc.* **2010**, *132*, 12847-12849.

62.   Shin, K.; Park, Y.; Baik, M.-H.; Chang, S. Iridium-catalysed arylation of C–H bonds enabled by oxidatively induced reductive elimination. *Nat. Chem.* **2017**, *10*, 218.

63.   Kim, J.; Shin, K.; Jin, S.; Kim, D.; Chang, S. Oxidatively Induced Reductive Elimination: Exploring the Scope and Catalyst Systems with Ir, Rh, and Ru Complexes. *J. Am. Chem. Soc.* **2019**, *141*, 4137-4146.

64.   Lanci, M. P.; Remy, M. S.; Kaminsky, W.; Mayer, J. M.; Sanford, M. S. Oxidatively Induced Reductive Elimination from (ᵗBu₂bpy)Pd(Me)₂: Palladium(IV) Intermediates in a One-Electron Oxidation Reaction. *J. Am. Chem. Soc.* **2009**, *131*, 15618-15620.

65.   Desnoyer, A. N.; Love, J. A. Recent advances in well-defined, late transition metal complexes that make and/or break C-N, C-O and C-S bonds. *Chem. Soc. Rev.* **2017**, *46*, 197-238.

66.   Young, K. J. H.; Mironov, O. A.; Periana, R. A. Stoichiometric Oxy Functionalization and CH Activation Studies of Cyclometalated Iridium(III) 6-Phenyl-2,2'-Bipyridine Hydrocarbyl Complexes. *Organometallics* **2007**, *26*, 2137-2140.

67.   Han, R.; Hillhouse, G. L. Carbon−Oxygen Reductive-Elimination from Nickel(II) Oxametallacycles and Factors That Control Formation of Ether, Aldehyde, Alcohol, or Ester Products. *J. Am. Chem. Soc.* **1997**, *119*, 8135-8136.

68.   Koo, K.; Hillhouse, G. L. Carbon-Nitrogen Bond Formation by Reductive Elimination from Nickel(II) Amido Alkyl Complexes. *Organometallics* **1995**, *14*, 4421-4423.

69. Cloutier, J.-P.; Zargarian, D. Functionalization of the Aryl Moiety in the Pincer Complex (NCN)Ni[III]Br$_2$: Insights on Ni[III]-Promoted Carbon–Heteroatom Coupling. *Organometallics* **2018**, *37*, 1446-1455.

70. Cloutier, J.-P.; Vabre, B.; Moungang-Soumé, B.; Zargarian, D. Synthesis and Reactivities of New NCN-Type Pincer Complexes of Nickel. *Organometallics* **2015**, *34*, 133-145.

71. Casitas, A.; King, A. E.; Parella, T.; Costas, M.; Stahl, S. S.; Ribas, X. Direct observation of Cu[I]/Cu[III] redox steps relevant to Ullmann-type coupling reactions. *Chem. Sci.* **2010**, *1*, 326-330.

72. Font, M.; Acuña-Parés, F.; Parella, T.; Serra, J.; Luis, J. M.; Lloret-Fillol, J.; Costas, M.; Ribas, X. Direct observation of two-electron Ag(I)/Ag(III) redox cycles in coupling catalysis. *Nat. Commun.* **2014**, *5*, 4373.

73. Casitas, A.; Ribas, X. The role of organometallic copper(III) complexes in homogeneous catalysis. *Chem. Sci.* **2013**, *4*, 2301-2318.

74. Khusnutdinova, J. R.; Rath, N. P.; Mirica, L. M. Stable Mononuclear Organometallic Pd(III) Complexes and Their C−C Bond Formation Reactivity. *J. Am. Chem. Soc.* **2010**, *132*, 7303-7305.

75. Wang, H.; Choi, I.; Rogge, T.; Kaplaneris, N.; Ackermann, L. Versatile and robust C–C activation by chelation-assisted manganese catalysis. *Nature Catalysis* **2018**, *1*, 993-1001.

76. Planas, O.; Whiteoak, C. J.; Martin-Diaconescu, V.; Gamba, I.; Luis, J. M.; Parella, T.; Company, A.; Ribas, X. Isolation of Key Organometallic Aryl-Co(III) Intermediates in Cobalt-Catalyzed C(sp^2)-H Functionalizations and New Insights into Alkyne Annulation Reaction Mechanisms. *J. Am. Chem. Soc.* **2016**, *138*, 14388-14397.

77. Planas, O.; Roldan-Gomez, S.; Martin-Diaconescu, V.; Parella, T.; Luis, J. M.; Company, A.; Ribas, X. Carboxylate-Assisted Formation of Aryl-Co(III) Masked-Carbenes in Cobalt-Catalyzed C-H Functionalization with Diazo Esters. *J. Am. Chem. Soc.* **2017**, *139*, 14649-14655.

78. Planas, O.; Roldan-Gomez, S.; Martin-Diaconescu, V.; Luis, J. M.; Company, A.; Ribas, X. Mechanistic insights into the S$_N$2-type reactivity of aryl-Co(III) masked-carbenes for C-C bond forming transformations. *Chem. Sci.* **2018**, *9*, 5736-5746.

79. Cipot, J.; Wechsler, D.; McDonald, R.; Ferguson, M. J.; Stradiotto, M. Synthesis and Crystallographic Characterization of New Manganese(I) Complexes of Donor-Functionalized Indenes. *Organometallics* **2005**, *24*, 1737-1746.

80. Cockman, R. W.; Hoskins, B. F.; McCormick, M. J.; O'Donnell, T. A. Isolation and crystal structure of manganese(II) tetrafluoroborate: a unique example of manganese(II) with seven unidentate ligands. *Inorg. Chem.* **1988**, *27*, 2742-5.

81. Bauer, J. A. K.; Becker, T. M.; Orchin, M. The preparation and crystal structures of a covalent tetrafluoroborato complex, (CO)$_3$(dppfe)MnFBF$_3$, and of a related ionic complex, [(CO)$_4$(dppfe)Mn]BF$_4$ [(dppfe) = bis(1,1'-diphenylphosphino)ferrocene]. *J. Chem. Crystallogr.* **2005**, *35*, 141-146.

82. Rybtchinski, B.; Oevers, S.; Montag, M.; Vigalok, A.; Rozenberg, H.; Martin, J. M. L.; Milstein, D. Comparison of Steric and Electronic Requirements for C-C and C-H Bond Activation. Chelating vs Nonchelating Case. *J. Am. Chem. Soc.* **2001**, *123*, 9064-9077.

83. Gudun, K. A.; Segizbayev, M.; Adamov, A.; Plessow, P. N.; Lyssenko, K. A.; Balanay, M. P.; Khalimon, A. Y. POCN Ni(II) pincer complexes: synthesis, characterization and evaluation of catalytic hydrosilylation and hydroboration activities. *Dalton Trans.* **2019**, *48*, 1732-1746.

84. Corcos, A. R.; Berry, J. F. Anilinopyridinate-supported Ru$_2$[x+] (x = 5 or 6) paddlewheel complexes with labile axial ligands. *Dalton Trans.* **2017**, *46*, 5532-5539.

85. Herbert, D. E.; Lara, N. C.; Agapie, T. Arene C-H Amination at Nickel in Terphenyl-Diphosphine Complexes with Labile Metal-Arene Interactions. *Chem. Eur. J.* **2013**, *19*, 16453-16460.

86. Wozniak, D. I.; Sabbers, W. A.; Weerasiri, K. C.; Dinh, L. V.; Quenzer, J. L.; Hicks, A. J.; Dobereiner, G. E. Comparing Interactions of a Three-Coordinate Pd Cation with Common Weakly Coordinating Anions. *Organometallics* **2018**, *37*, 2376-2385.

87. See Supporting Information for details.

88. In the cases of **1** and **2**, a substitutional N1/C1 ligand disorder occurs .

89. Forniés, J.; Martín, A.; Martín, L. F.; Menjón, B.; Zhen, H.; Bell, A.; Rhodes, L. F. The First Structurally Characterized Homoleptic Aryl-Manganese(III) Compound and the Corresponding Isoleptic and Isoelectronic Chromium(II) Derivative. *Organometallics* **2005**, *24*, 3266-3271.

90. Morris, R. J.; Girolami, G. S. High-valent organomanganese chemistry. 2. Synthesis and characterization of manganese(III) aryls. *Organometallics* **1991**, *10*, 799-804.

91. Morris, R. J.; Girolami, G. S. Isolation and characterization of the first sigma-organomanganese(III) complex. Crystal and molecular structure of (2,4,6-trimethylphenyl)dibromobis(trimethylphosphine)manganese(III). *Organometallics* **1987**, *6*, 1815-1816.

92. Dey, K.; De, R. L. Organometallic derivatives of cobalt(III), chromium(III) and manganese(III) complexes of Schiff bases. *J. Inorg. Nucl. Chem.* **1977**, *39*, 153-155.

93. Iwata, Y.; Tanaka, Y.; Kubosaki, S.; Morita, T.; Yoshimi, Y. A strategy for generating aryl radicals from arylborates through organic photoredox catalysis: photo-Meerwein type arylation of electron-deficient alkenes. *Chem. Commun.* **2018**, *54*, 1257-1260.

94. Tokmakov, I. V.; Kim, G.-S.; Kislov, V. V.; Mebel, A. M.; Lin, M. C. The Reaction of Phenyl Radical with Molecular Oxygen: A G2M Study of the Potential Energy Surface. *J. Phys. Chem. A* **2005**, *109*, 6114-6127.

95. Santilli, C.; Beigbaghlou, S. S.; Ahlburg, A.; Antonacci, G.; Fristrup, P.; Norrby, P.-O.; Madsen, R. The Manganese-Catalyzed Cross-Coupling Reaction and the Influence of Trace Metals. *Eur. J. Org. Chem.* **2017**, *2017*, 5269-5274.

96. Heyduk, A. F.; Nocera, D. G. Hydrogen Produced from Hydrohalic Acid Solutions by a Two-Electron Mixed-Valence Photocatalyst. *Science* **2001**, *293*, 1639.

97. Fu, N.; Sauer, G. S.; Lin, S. Electrocatalytic Radical Dichlorination of Alkenes with Nucleophilic Chlorine Sources. *J. Am. Chem. Soc.* **2017**, *139*, 15548-15553.

98. Carrera, E. I.; McCormick, T. M.; Kapp, M. J.; Lough, A. J.; Seferos, D. S. Thermal and Photoreductive Elimination from the Tellurium Center of π-Conjugated Tellurophenes. *Inorg. Chem.* **2013**, *52*, 13779-13790.

99. Teets, T. S.; Nocera, D. G. Halogen Photoreductive Elimination from Gold(III) Centers. *J. Am. Chem. Soc.* **2009**, *131*, 7411-7420.

100. Perera, T. A.; Masjedi, M.; Sharp, P. R. Photoreduction of Pt(IV) Chloro Complexes: Substrate Chlorination by a Triplet Excited State. *Inorg. Chem.* **2014**, *53*, 7608-7621.

101. Zhang, Z.-F.; Su, M.-D. The mechanistic investigations of photochemical carbonyl elimination and oxidative addition reactions of (η^5-C$_5$H$_5$)M(CO)$_3$, (M = Mn and Re) complexes. *RSC Adv,* **2018**, *8*, 10987-10998.

102. Connelly, N. G.; Geiger, W. E. Chemical Redox Agents for Organometallic Chemistry. *Chem. Rev.* **1996**, *96*, 877-910.

103. Shields, B. J.; Doyle, A. G. Direct C(sp^3)–H Cross Coupling Enabled by Catalytic Generation of Chlorine Radicals. *J. Am. Chem. Soc.* **2016**, *138*, 12719-12722.

104. Smoukov, S. K.; Telser, J.; Bernat, B. A.; Rife, C. L.; Armstrong, R. N.; Hoffman, B. M. EPR Study of Substrate Binding to the Mn(II) Active Site of the Bacterial Antibiotic Resistance Enzyme FosA: A Better Way To Examine Mn(II). *J. Am. Chem. Soc.* **2002**, *124*, 2318-2326.

105. McQuarrie, D. A.; Cox, H.; Simon, J. D.; Choi, J. *Physical Chemistry: A Molecular Approach*. University Science Books: 1997.

106. Sheldrick, G. M. SHELXT - Integrated space-group and crystal-structure determination. *Acta Crystallogr., Sect. A: Found. Adv.* **2015**, *71*, 3-8.

107. Sheldrick, G. M. Crystal structure refinement with SHELXL. *Acta Crystallogr., Sect. C: Struct. Chem.* **2015**, *71*, 3-8.

108.   Farrugia, L. J. WinGX and ORTEP for Windows: an update. *J. Appl. Crystallogr.* **2012,** *45*, 849-854.

109.   Dolomanov, O. V.; Bourhis, L. J.; Gildea, R. J.; Howard, J. A. K.; Puschmann, H. OLEX2: a complete structure solution, refinement and analysis program. *J. Appl. Crystallogr.* **2009,** *42*, 339-341.

110.   Spek, A. L. PLATON SQUEEZE: a tool for the calculation of the disordered solvent contribution to the calculated structure factors. *Acta Crystallogr., Sect. C: Struct. Chem.* **2015,** *71*, 9-18.

111.   Parsons, S.; Flack, H. D.; Wagner, T. Use of intensity quotients and differences in absolute structure refinement. *Acta Crystallogr., Sect. B* **2013,** *69*, 249-259.

112.   Flack, H. D.; Bernardinelli, G. Reporting and evaluating absolute-structure and absolute-configuration determinations. *J. Appl. Crystallogr.* **2000,** *33*, 1143-1148.